

Research paper

Enhanced brain targeting by synthesis of 3',5'-dioctanoyl-5-fluoro-2'-deoxyuridine and incorporation into solid lipid nanoparticles

Jian-Xin Wang^a, Xun Sun^b, Zhi-Rong Zhang^{b,*}^aShanghai Institute of Chinese Materia Medica, Shanghai, People's Republic of China^bWest China School of Pharmacy, Sichuan University, Chengdu, People's Republic of China

Received 13 December 2001; accepted in revised form 5 June 2002

Abstract

To overcome the limited access of the drug 5-fluoro-2'-deoxyuridine (FUdR) to the brain, 3',5'-dioctanoyl-5-fluoro-2'-deoxyuridine (DO-FUdR) was synthesized and incorporated into solid lipid nanoparticles (DO-FUdR-SLN). DO-FUdR-SLN were prepared by a thin-layer ultrasonication technique and a central composite design (CCD) was applied to optimize the formulation. The median particle size of DO-FUdR-SLN was 76 nm with drug loading of 29.02% and entrapment efficiency of 96.62%. The in vitro drug release was studied by a bulk-equilibrium reverse dialysis bag technique in phosphate-buffered saline (pH 7.4) containing 0.3% pancreatic enzyme at 37°C. The concentrations of FUdR in various organs were determined by reversed-phase high-performance liquid chromatography after intravenous administration of DO-FUdR-SLN, DO-FUdR or FUdR. The brain area under the concentration–time curve of DO-FUdR-SLN and DO-FUdR were 10.97- and 5.32-fold higher than that of FUdR, respectively. These results indicated that DO-FUdR-SLN had a good brain targeting efficiency in vivo. SLN can improve the ability of the drug to penetrate through the blood–brain barrier and is a promising drug targeting system for the treatment of central nervous system disorders. © 2002 Elsevier Science B.V. All rights reserved.

Keywords: 3',5'-Dioctanoyl-5-fluoro-2'-deoxyuridine; Solid lipid nanoparticles; Brain targeting

1. Introduction

Biodegradable polymers from natural and synthetic sources have been widely used in the production of nanoparticles. A certain advantage of polymer-based nanoparticles is the wealth of possible chemical modifications, including the synthesis of block- and comb-polymers. However, problems of polymer-based nanoparticles derive from residues from organic solvents used in the production process, polymer cytotoxicity and the scaling up of the production processes [1]. Recently, increasing attention has been focused on solid lipid nanoparticles (SLN), because it has advantages of the traditional colloidal systems but avoids some of their major disadvantages [2]. Proposed advantages include: possibility of controlled drug release and drug targeting, increased drug stability, high drug payload, no biotoxicity of the carriers, avoidance of organic solvents, no problems with respect to large scale production and sterilization. Furthermore, SLN can

decrease the uptake of the drug by the mononuclear phagocyte system, therefore, prolong the lifetime of the drug in circulation and increase the targeting potential of the drug.

The pharmacological treatment of central nervous system (CNS) diseases, such as brain tumors, AIDS, neurological and psychiatric disorders, is often confined by the inability of potent drugs to pass the blood–brain barrier (BBB), which is formed by the endothelium of the brain vessels, the basal membrane and neuroglial cells. It is widely accepted that only compounds, which are unionized at physiological pH, lipophilic and of low molecular weight can cross the BBB. 5-Fluoro-2'-deoxyuridine (FUdR), a derivative of 5-fluorouracil (FU), is an anti-metabolite and shows a significant cytotoxic activity. This drug is widely used for the treatment of some solid tumors of, for example, the liver, brain, breast, colon and rectum. However, it is rapidly metabolized after administration, particularly by the liver. The anti-tumor effect of FUdR depends markedly upon the duration of the exposure of tumor cells to the drug. The rather short half-life of FUdR in vivo reduces its pharmacological effect.

To investigate the specific brain targeting of FUdR, we synthesized an esterified prodrug 3',5'-dioctanoyl-5-fluoro-2'-deoxyuridine (DO-FUdR) and incorporated it into SLN

* Corresponding author. West China School of Pharmacy, Sichuan University, Chengdu 610041, People's Republic of China.
Tel.: +86-28-85501566; fax: +86-28-85456898.

E-mail address: zrzzl@mail.sc.cninfo.net (Z.-R. Zhang).

[3,4]. After studying the characteristics of DO-FuDR-SLN and its in vitro drug release, we assessed the feasibility of DO-FuDR-SLN in prolonging drug release and in achieving in vivo specific brain targeting via the intravenous (i.v.) route. The concentrations of FuDR in organs and in plasma were determined after i.v. administration of DO-FuDR-SLN in mice by using reversed-phase high-performance liquid chromatography (HPLC). In addition, the biodistribution of free and SLN encapsulated FuDR were compared.

2. Experimental

2.1. Materials

FuDR was supplied by Haizheng Pharmaceutical Corporation (Zhejiang, People's Republic of China); octanoic acid by Chengdu reagent Company (Chengdu, People's Republic of China); Pluronic F-68 and Pluronic F-127 by Sigma. All the other chemicals and reagents used were of the analytical grade obtained commercially.

2.2. Synthesis of DO-FuDR

Octanoic acid 3.95 ml (0.025 mol) and thionyl chloride 2.75 ml (0.0375 mol) were added into a dry flask and were stirred for 4 h at room temperature. The excess thionyl chloride was removed by evaporation under vacuum. The residuum was reserved for later reaction. FuDR, 2.462 g (0.01 mol) was dissolved in 50 ml of anhydrous pyridine and were cooled to 4°C. Then this liquid was mixed with the above residuum by stirring with low speed at room temperature for 12 h. Afterwards, the reaction solution was poured into iced water and extracted three times with equal volumes of chloroform. The chloroform was then washed twice with each of 0.01 N H₂SO₄, 1% NaHCO₃ and finally distilled water. After drying with anhydrous calcium sulphate, the chloroform was evaporated under reduced pressure. The residuum was purified by fast silica gel column chromatography (eluting solvent system, petroleum ether/ether 5:1) and a yellow oily liquid 4.61 g was obtained at a 92.5% overall yield [5].

2.3. Preparation of DO-FuDR-SLN

Emulsion-precipitation, melt-homogenization and thin-layer ultrasonication techniques were studied to prepare DO-FuDR-SLN and the thin-layer ultrasonication technique was preferred. Central composite design (CCD) was applied to the optimization of the formulation [6,7]. The ratio of drug and lecithin (D:L), the concentration of F-68 and the concentration of glycerol tristearate (GTS), which are the most influential factors, were optimized taking the average particle size, the entrapment efficiency and the drug loading as indexes. The experimental results were fitted to a binomial equation. According to the regression equation, the response surfaces, which describe the relationship between

each index and each factor, were drawn to select the optimum ingredient composition. The preferred conditions were found to be D:L 0.7, 3% F-68 and 0.5% GTS [8]. The preparation procedure was as follows. DO-FuDR, lecithin and GTS were dissolved in dichloromethane and concentrated under vacuum to a constant weight. A thin even lipid film was formed by rotary evaporation using a round-bottomed flask and vacuum-desiccated at room temperature overnight to remove residual traces of organic solvents. An appropriate amount of aqueous solution of Pluronic F-68 was added into the flask and the mixture was sonicated using a Sonifier Cell Disruptor equipped with a microprobe for 3 min. The DO-FuDR-SLN were obtained and stored at 4°C.

2.4. Morphology and particle size

DO-FuDR-SLN were examined by transmission electron microscopy (JEM-100SX, Japan). Samples were prepared by placing a drop of DO-FuDR-SLN suspension onto a copper grid and air-drying, followed by negative staining with a drop of 2% aqueous solution of sodium phosphotungstate for contrast enhancement. The air-dried samples were then directly examined under the transmission microscope. The particle size of DO-FuDR-SLN was determined by a laser particle analyzer (Master 2000, Malvern).

2.5. Determination of drug loading and entrapment efficiency

The DO-FuDR-SLN suspension was separated by dextran-gel column chromatography. The concentrations of DO-FuDR in the suspension and in SLN were assayed by reversed phase HPLC after dilution with methanol.

2.6. Drug release of DO-FuDR-SLN

In vitro release was evaluated using a bulk-equilibrium reverse dialysis bag technique. The dissolution medium was composed of 0.3% trypsinogen and phosphate-buffered saline (PBS, 0.1 M, pH 7.4). FuDR solution, 1 ml, DO-FuDR suspension (1.24% solids in the suspension) or DO-FuDR-SLN suspension (6.50% solids in the suspension) was directly added to 200 ml of dissolution medium, respectively, where 12 dialysis bags containing 1 ml of the same dissolution medium were previously immersed. It should be emphasized that the dialysis sacs were equilibrated with the dissolution medium for a few hours prior to the experiments. The release kinetic experiments were performed at a fixed temperature of 37°C under constant magnetic stirring. At predetermined time intervals, the dialysis sacs were withdrawn from the stirred release solution, and the content of the sacs was assayed for FuDR by HPLC.

2.7. Body distribution of DO-FuDR-SLN

The Sichuan University animal ethical experimentation committee, according to the requirements of the National

Act on the use of experimental animals (People's Republic of China) approved all procedures of the *in vivo* studies. Kunming mice, body weight between 18 and 22 g, female or male were provided by the Laboratory Animal Center of West China University of Medical Sciences. The DO-FuDR-SLN, DO-FuDR and FuDR-Sol were injected *i.v.* into the tail vein of the mice. For each preparation and each sampling time point, five mice were treated with a single dose equivalent to 20 mg/kg FuDR (0.1 ml/10 g body weight). The mice were anesthetized by inhalation of diethyl ether before blood sample collection.

At the predetermined time, blood samples were collected from the ocular artery directly after eyeball removal and placed into test tubes containing 10 μ l of heparin solution. Plasma was immediately separated by centrifugation. The animals were dissected and each tested organ (heart, liver, spleen, lung, kidney and brain) was removed. Every organ sample was accurately weighed and homogenized.

The extraction procedure was as follows. Plasma (0.5 ml) or homogenized tissue (0.5 g) was mixed with 0.1 ml acyclovir (20 mg/l) as the internal standard solution. The mixture was shaken with 3 ml ethyl acetate for 3 min on a vortexer and after centrifugation at $9000 \times g$ for 10 min, the organic layer was transferred to a test tube. The residual water layer and precipitants were subjected to re-extraction with 3 ml ethyl acetate. After centrifugation, the organic layer was combined with the first organic layer and the combined extract was evaporated to dryness under nitrogen gas at room temperature. Dried samples were dissolved in 0.1 ml methanol and centrifuged at $9000 \times g$ for 10 min. Then 20 μ l clear supernatants were injected into the HPLC.

2.8. Analysis method

The HPLC assay methods were established for determination of the concentrations of the FuDR, its prodrug DO-

FuDR, and FuDR in plasma or tissue. A Shimpack CLC-ODS C_{18} column (5 μ m, 150 mm \times 4.6 mm, ID), was used. The UV detector was operated at 265 nm. The analysis was performed at a temperature of 30°C and a flow rate of 1.0 ml/min. In the analysis of FuDR, the mobile phase was composed of 95% 0.1 M (pH 7.4) phosphate buffer solution–methanol. For DO-FuDR, the mobile phase was composed of methanol–pH 4.0 phosphate buffer solution (v/v, 75:25), while for the assay of FuDR in plasma or tissue, ammonium biphosphate buffer solution (0.05 M, pH 3.2)–methanol (v/v, 98:2) was employed as the eluent.

2.9. Pharmacokinetic analysis

Plasma and tissue concentration data of FuDR obtained from mice were pooled to provide mean concentration data. The pharmacokinetics of FuDR was described as a two-compartment open model. The pharmacokinetic parameters in plasma and organs were obtained as follows. The area under the concentration–time curve (AUC) was calculated using the linear trapezoidal rule and extrapolated to infinity by dividing the last measurable concentration by the elimination rate constant. Mean residence time (MRT) was calculated by statistic moment program. Overall targeting efficiency (TE^C), targeting index (TI^C) and relative overall targeting efficiency (RTE^C) of DO-FuDR-SLN were calculated and compared with those of FuDR solution to evaluate the brain targeting property of DO-FuDR-SLN [9]. Overall targeting efficiency (TE^C) can be calculated as

$$TE^C = \frac{(AUC_{0 \rightarrow \infty})_i}{\sum_{i=1}^n (AUC_{0 \rightarrow \infty})_i} \times 100\%$$

where the denominator refers to the sum total of drug exposure to all the tissues, including the target tissue.

$$TI^C = \frac{(AUC_{0 \rightarrow \infty})_{DO-FuDR-SLN}}{(AUC_{0 \rightarrow \infty})_{FuDR-Sol}}$$

$$RTE^C = \frac{TE^C_{DO-FuDR-SLN} - TE^C_{FuDR-Sol}}{TE^C_{FuDR-Sol}} \times 100\%$$

3. Results and discussion

3.1. Structure and character determination of DO-FuDR

The structure of DO-FuDR was confirmed by mass spectrometry and IR spectrophotometry and detailed by 1H and ^{13}C NMR studies.

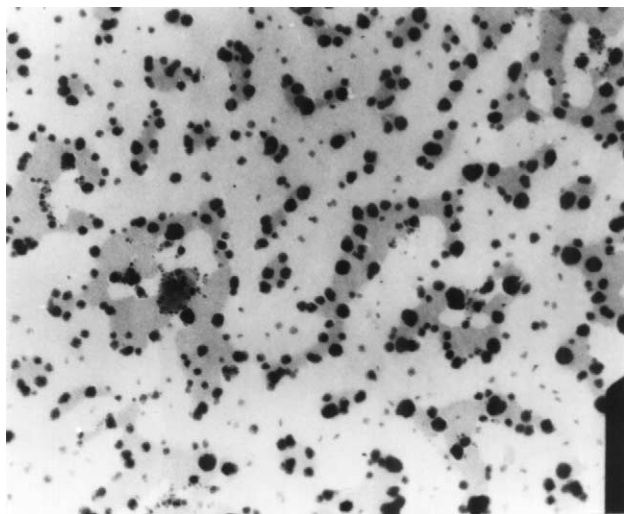
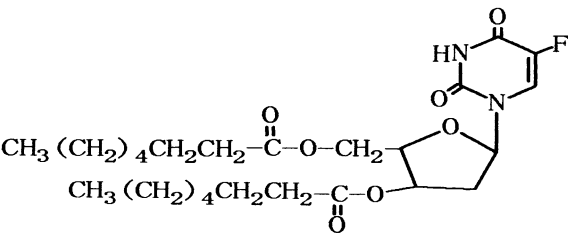


Fig. 1. Microphotograph of DO-FuDR-SLN by transmission electron microscopy ($\times 20,000$).

Table 1
The entrapment efficiency and drug loading of DO-FuDR in DO-FuDR-SLN (*n* = 3)

No.	EE ± RSD (%)	DL ± RSD (%)
1	96.68 ± 1.24	29.13 ± 0.55
2	95.29 ± 1.36	28.71 ± 0.48
3	97.01 ± 1.31	29.23 ± 0.67



The aqueous solubility of the compound in PBS (pH 7.4) at 37.0 ± 0.5°C was found to be 27.5 ± 1.1 µg/ml (5.52 × 10⁻⁵ M). The lipophilicity of DO-FuDR was assessed by the shake-flask method and the partition coefficient between chloroform and PBS (pH 7.4) was found to be 32451, i.e. log *P* = 4.51 ± 0.52. The degradation rate constant in PBS (pH 7.4) of DO-FuDR was 0.00187 h⁻¹ and its hydrolysis was found to occur in buffers (pH range 2–9). The fastest rate of enzymatic hydrolysis of DO-FuDR was observed in 10% plasma and 4% tissue homogenate and was found to follow apparent first order hydrolysis kinetics.

3.2. Nanoparticle characterization

Transmission electron microscopy demonstrated a regular spherical surface for DO-FuDR-SLN (Fig. 1)
The average diameter of DO-FuDR-SLN was 76 nm and 75% particles were less than 105 nm. The entrapment efficiency and drug loading are shown in Table 1.
The loading capacity of SLN was found to be satisfacto-

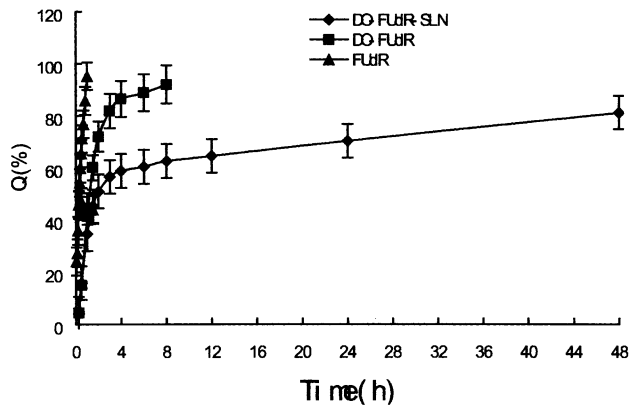


Fig. 2. The release curve of FuDR from FuDR solution, DO-FuDR and DO-FuDR-SLN (*n* = 3).

Table 2
Pharmacokinetic parameters of FuDR in mice after i.v. administration of DO-FuDR-SLN, DO- FuDR or FuDR solution

Parameters	FuDR solution	DO-FuDR	DO-FuDR-SLN
A (µg ml ⁻¹)	41.34	22.53	22.70
B (µg ml ⁻¹)	12.81	3.31	3.06
α (h ⁻¹)	6.33	0.86	0.42
β (h ⁻¹)	0.34	0.105	0.036
<i>t</i> _{1/2} α (h)	0.11	0.802	1.66
<i>t</i> _{1/2} β (h)	2.06	6.62	19.04
<i>K</i> ₂₁ (h ⁻¹)	1.76	0.202	0.082
<i>K</i> ₁₀ (h ⁻¹)	1.22	0.49	0.19
<i>K</i> ₁₂ (h ⁻¹)	3.70	0.32	0.19
AUC (h mg ml ⁻¹)	44.54	57.72	138.36
MRT (h)	2.58	5.33	15.85

rily high. Entrapment efficiency and drug loading of nanoparticles were determined using dextran-gel column chromatography.

3.3. In vitro release

Fig. 2 shows the FuDR release profile from FuDR solution, DO-FuDR and DO-FuDR-SLN.
The FuDR release profile from DO-FuDR-SLN can be characterized by a bioexponential equation: 1 – *Q* = 1.040 6e^{-0.4131t} + 0.4444e^{-0.0179t} (*r*₁ = 0.9903, *r*₂ = 0.9995) γ² = 0.9992 (Akaike Information Criterion) AIC = –63.984.
The release of FuDR from DO-FuDR-SLN was drastically delayed as a result of an increase in the lipophilicity of the prodrug and the incorporation of the prodrug into SLN. In the design of colloidal drug-carrier formulations, it is of vital importance to study the rate at which the drug is released from the carrier. Dynamic dialysis is a widely used method for measuring drug release. But in this method, the colloidal suspension is never diluted, and the experiment is not performed under sink conditions even if such conditions are constantly maintained in the acceptor compartment where sampling is performed. Consequently, the method

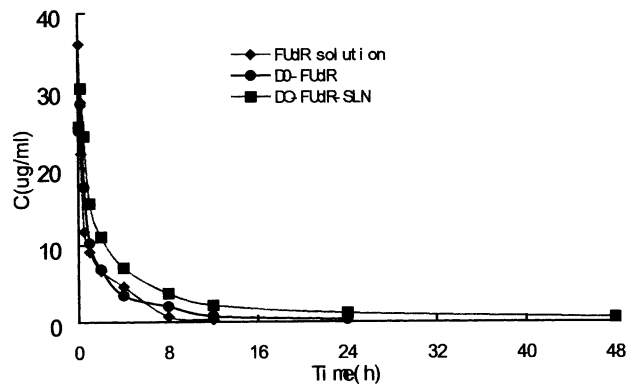


Fig. 3. Plasma concentration–time curves of FuDR after i.v. administration of FuDR solution, DO-FuDR or DO-FuDR-SLN (20 mg kg⁻¹).

Table 3

Concentration of FUDR in brain after i.v. administration of FUDR solution or DO-FUDR-SLN in mice ($\mu\text{g/g}$)

Time (h)	0.083	0.25	0.5	1	2	4	8	12	24	48	72
FUDR solution	7.87	5.61	4.37	3.95	3.16	1.48	0.73	0.58	0.36	/	/
DO-FUDR	19.21	20.86	21.12	12.84	10.45	7.81	5.59	3.05	1.41	0.67	0.34
DO-FUDR-SLN	21.15	26.64	22.83	15.86	13.12	10.34	7.90	5.52	4.37	2.64	1.03

does not measure the true release rate but rather the partition of a drug between the various phases of a dispersed system [10]. In the bulk-equilibrium reverse dialysis bag technique, the colloidal drug carrier suspension is directly placed in the release solution where it has the opportunity to release the drug load under maximum dilution (perfect sink conditions) [11]. Therefore, the nanoparticles displaying a considerable large interfacial area are directly exposed to the extended sink volume solution reflecting a natural biological environment. Drug will therefore diffuse out from the nanoparticles to the sink solution according to a true and real gradient existing between the nanoparticles and the regenerated apparent aqueous phase. Drug dissolved in the aqueous phase will easily diffuse through the sink solution into the dialysis bags. The percent drug release was calculated from the ratio of drug concentration measured at predetermined time intervals in the dialysis bags vs. the total concentration of the drug in the sink solution.

From the release profiles, it may be conjectured that since the outer shell of SLN was composed of lecithin, (and) quite a lot of drug, was released in the form of a burst. The core of SLN mainly consisted of GTS and a portion of drug, was released more gradually. However, the characterization of the molecular arrangement of the drug and the lipid needs to be further investigated by NMR and ESR techniques.

3.4. Body distribution and pharmacokinetic study in mice

Table 2 shows the pharmacokinetic parameters of FUDR in mice after i.v. administration of FUDR solution, DO-FUDR or DO-FUDR-SLN.

Fig. 3 displays the plasma drug level vs. time curves after administration of FUDR solution, DO-FUDR or DO-FUDR-SLN.

Table 3 reports the concentration of FUDR after administration of FUDR, DO-FUDR or DO-FUDR-SLN solution in mice.

Table 4

Pharmacokinetic parameters of FUDR (calculated by statistical moments) in brain tissue after i.v. administration of DO-FUDR-SLN, DO-FUDR or FUDR solution to mice

Parameter	FUDR solution	DO-FUDR	DO-FUDR-SLN
AUC (h $\mu\text{g/g}$)	31.65	168.52	347.11
MRT (h)	12.32	20.94	31.14
$t_{1/2}$ (h)	8.54	14.51	21.58

Table 4 shows the pharmacokinetic parameters of FUDR calculated by moment in brain tissue after i.v. administration of DO-FUDR-SLN, DO-FUDR or FUDR to mice.

Table 5 presents the overall targeting efficiency of DO-FUDR-SLN and FUDR solution.

Table 6 provides the comparison of targeting parameters between DO-FUDR-SLN and FUDR solution.

From the above tables and figures, it was evident that there existed significant differences between FUDR and DO-FUDR-SLN. Compared with FUDR solution, the brain targeting efficiency of DO-FUDR-SLN was greatly improved. The brain AUC of DO-FUDR-SLN was 10.97-fold greater. The overall drug targeting efficiency (TE^{C}) was enhanced from 11.77 to 29.81%, leading to a prolonged $t_{1/2}$ value in the brain from 8.54 to 21.58 h. Meanwhile, the AUC in the brain of DO-FUDR-SLN was 2.06-fold higher than DO-FUDR and the $t_{1/2}$ value in brain was 1.49-fold longer. Therefore, it could be deduced that the increased lipophilicity of the prodrug DO-FUDR played a rather important role in increasing the brain targeting efficiency of DO-FUDR-SLN. DO-FUDR enables a better penetration and transport into and across the lipophilic endothelial barrier and/or of a circumvention of the efflux-pump systems [12]. However, the following reasons also contribute to the noticeable enhancement of CNS distribution. Firstly, the surface modification of SLN by Pluronic F-68 could cause steric hindrance effect to decrease the adsorption of opsonin to SLN in plasma, which could retard the rapid removal of particles by the reticuloendothelial system (RES) and prolong the retention time of SLN in plasma [13,14]. Secondly, an increased retention of the DO-FUDR-SLN in the brain blood capillaries is combined with an adsorption to the capillary walls. This could create a higher concentration gradient that would enhance the transport across the endothelial cell layer and as a result the delivery to the brain [15,16]. Furthermore, the DO-FUDR-SLN may be endocytosed by the endothelial cells followed by the release of the drugs within these cells and delivery to the brain [12,17].

Table 5

Overall targeting efficiency (TE^{C}) of DO-FUDR-SLN and FUDR solution

Tissue	Plasma	Heart	Liver	Spleen	Lung	Kidney	Brain
FUDR solution	17.93	18.66	22.65	9.72	8.72	10.57	11.77
DO-FUDR-SLN	11.94	7.78	25.93	9.33	9.79	5.40	29.84

Table 6

Comparison of targeting parameters between DO-FuDR-SLN and FuDR solution

Tissue	Plasma	Heart	Liver	Spleen	Lung	Kidney	Brain
TI ^C	2.88	1.80	4.95	4.15	4.85	2.21	10.97
RTE ^C (%)	−33.41	−58.30	14.48	−3.99	12.25	−48.92	153.65

Acknowledgements

The study was sponsored by the National Natural Fund for Distinguished Young Scholars of People's Republic of China.

References

- [1] W. Mehnert, K. Mäder, Solid lipid nanoparticles: production, characterization and applications, *Adv. Drug Deliv. Rev.* 47 (2001) 165–196.
- [2] R.H. Muller, K. Mader, S. Gohla, Solid lipid nanoparticles (SLN) for controlled drug delivery – a review of the art, *Eur. J. Pharm. Biopharm.* 50 (2000) 161–177.
- [3] N. Oshihiko, E.C. John, 3',5'-diesters of 5-fluoro-2'-deoxyuridine: synthesis and biological activity, *Biochem. Pharmacol.* 14 (1965) 1605–1619.
- [4] F. Shoji, K. Takeo, N. Mika, Selective antiancer effects of 3',5'-dioctanoyl-5-fluoro-2'-deoxyuridine, a lipophilic prodrug of 5-fluoro-2'-deoxyuridine dissolved in an oily lymphographic agent on hepatic cancer of rabbits bearing VX-2 tumor, *Cancer Res.* 47 (1987) 1930–1934.
- [5] Y. Nishizawa, J.E. Casida, S.W. Anderson, C. Heidelberger, 3',5'-diesters of 5-fluoro-2'-deoxyuridine: synthesis and biological activity, *Biochem. Pharmacol.* 14 (1965) 1605–1619.
- [6] J. Molpeceres, M. Guzman, M.R. Aberturas, M. Chacon, L. Berges, Application of central composite designs to the preparation of polycaprolactone nanoparticles by solvent displacement, *J. Pharm. Sci.* 85 (1996) 206–213.
- [7] A.D. Mcleod, F.C. Lam, P.K. Gupta, C.T. Hung, Optimized synthesis of polyglutaraldehyde nanoparticles using central composite design, *J. Pharm. Sci.* 77 (1988) 704–710.
- [8] Z.R. Zhang, J.X. Wang, J. Lu, Optimization of the preparation of 3',5'-dioctanoyl-5-fluoro-2'-deoxyuridine pharmacosomes using central composite design, *Acta Pharm. Sinica* 36 (2001) 461–465.
- [9] Y.X. Peng, Y.L. Zhuang, G.T. Liao, Study on bone marrow targeting daunorubicin polybutylcyanoacrylate nanoparticles, *Chin. J. Pharm.* 31 (2000) 57–61.
- [10] C. Washington, Evaluation of non-sink dialysis methods for the measurement of drug release from colloids: effects of drug partition, *Int. J. Pharm.* 56 (1989) 71–74.
- [11] M.Y. Levy, S. Benita, Drug release from submicronized o/w emulsion: a new in vitro kinetic evaluation model, *Int. J. Pharm.* 66 (1990) 29–37.
- [12] J. Kreuter, Nanoparticulate systems for brain delivery of drugs, *Adv. Drug Deliv. Rev.* 47 (2001) 65–81.
- [13] S.M. Moghimi, Mechanisms regulating body distribution of nanospheres conditioned with pluronic and tetronic block co-polymers, *Adv. Drug Deliv. Rev.* 16 (1995) 183–186.
- [14] V. Lenaerts, A. Labib, F. Chouinard, Nanocapsules with a reduced liver uptake: targeting of phthalocyanines to EMT-6 mouse mammary tumor in vitro, *Eur. J. Pharm. Biopharm.* 41 (1995) 38–41.
- [15] J. Kreuter, R.N. Alyautdin, D.A. Kharkevich, A.A. Ivanov, Passage of peptides through the blood–brain barrier with colloidal polymer particles (nanoparticles), *Brain Res.* 674 (1995) 171–174.
- [16] S. Ulrike, S. Petra, U. Sven, B.A. Sabel, Nanoparticle technology for delivery of drugs across the blood–brain barrier, *J. Pharm. Sci.* 87 (1998) 1305–1307.
- [17] R. Alyautdin, D. Gothier, V. Petrov, Analgesic activity of the hexapeptide dalargin adsorbed on the surface of polysorbate 80-coated poly (butylcyanoacrylate) nanoparticles, *Eur. J. Pharm. Biopharm.* 41 (1995) 44–48.